Differential cross sections for elastic electron scattering. Charge-cloud polarization in H_2 †

M. Fink
Physics Department and Electronics Research Center, University of Texas, Austin, Texas 78712

K. Jost and D. Herrmann
Physikalisches Institut, Westfälische Wilhelms Universität, Münster, Germany

(Received 23 December 1974)

Relative elastic differential cross sections for electrons scattered from H_2 have been measured for angles between 3 and 130 deg and electron energies between 100 and 1000 eV. The data agree very well with the first Born theory by Ford and Browne, and Liu and Smith for angles larger than 30 deg; however, strong deviations are found in the small-angle range. This discrepancy is discussed from the point of view of charge-cloud polarization and its adiabatic limit. It was found that the cross sections have not yet reached the adiabatic limit at 100 eV. The differential cross sections are integrated, and the total elastic cross sections are determined. The present values continue smoothly to the results of Truhlar *et al.* and are compatible with those of Ulsh, Wellenstein, and Bonham.

I. INTRODUCTION

During the last ten years, a large variety of elastic differential cross sections [hereafter called $\sigma(\theta)$ or DCS] of many atoms and some molecules have been reported, mostly within the angular range of about 30–150°.[1-3]

The lack of sufficient precision and of small-angle measurements, however, has prevented a comprehensive study of the deformation of the electronic charge cloud under the influence of the incoming electrons. Nevertheless, the scattering process at high electron energies (producing no distortion) and at low energies (adiabatic distortion) is rather well understood, especially for helium.[4-6] However, there is little knowledge about the range of validity of both these approximations and about the intermediate range, where time- and energy-dependent scattering theory is required. In order to study these dynamic effects, a set of elastic $\sigma(\theta)$ curves at several energies between 100 and 1000 eV was desirable with special emphasis on the small-angle range and high density of data points.

Although there have been several accurate experiments reported for small-angle scattering, the collected information is currently not complete enough to establish a comprehensive picture of the charge cloud polarization mechanism. The shortcomings are as follows: first, most of the experimental data has been collected for helium[7-10]; second, too few electron energies have been investigated; and third, the data points are generally coarsely spaced. To overcome these deficiencies, a new scattering unit was built in order to measure an internally consistent set of $\sigma(\theta)$ curves for all the rare gases up to Xe and for selected molecules. The energy range chosen was 100–1000 eV, and the angular range was 3–135°. In this paper, only the H_2 results and a description of the unit will be presented. The $\sigma(\theta)$ curves of the other gases will be discussed in future presentations.

In Sec. II the general arrangement of the scattering unit is explained; in Sec. III the various subunits will be discussed in detail. Section IV contains the calibration and adjustment procedures and describes the uncertainties in the data, and in Secs. V and VI the present data will be compared with previous experimental work and with current theoretical results.

II. ARRANGEMENT OF THE SCATTERING UNIT

In most previous experiments, the recorded $\sigma(\theta)$ curves have been restricted to angles larger than 30° because the measurement utilized scattering volumes which were defined by the electron beam and the acceptance cone of the detector system. Thus, the scattering volume changed with the scattering angle. At wide angles (>30°), a simple "sine correction" factor compensates for this variation, providing the electron beam and the scattered electrons travel through completely field-free regions to guarantee straight trajectories. At small angles this correction becomes far more complicated, and the sensitivity for residual stray fields is greatly enhanced.[11] Several experiments have been reported where extended scattering volumes have been used and corrections into smallest angles have been applied. However, those studies did not take into consideration the influence of the stray fields; thus, a reconfirmation of that previous data and its extension were necessary.

These complications with the accompanying uncertainties of extended scattering volumes can be

avoided when the scattering volume is defined by the intersection of an electron beam and gas jet and when this volume is totally enclosed in the acceptance cone of the detection system[12] (see Sec. III). Therefore, it was decided to construct a crossed-beam unit. The advantage of this arrangement is that the angular range is restricted only by the width of the beam stop in the forward direction and by the size of the electron gun in the backward direction. Large-angle data are essential, since the geometry of the gas jet and its density could not be determined precisely enough to evaluate the differential cross section on an absolute scale. There are no absolute, experimental, large-angle $\sigma(\theta)$ values available for H_2. However, two sets of absolute data for He are known, and in the large-angle limit (>30°) in the energy range above 100 eV, the calculated $\sigma(\theta)$ values based on static scattering potentials agree very well with absolute experimental results at large angles.[7,9,13] For other targets we expect a similar agreement. Therefore, the data recorded with the present unit were matched at 90° to the predictions of the "static" potential theory. The experimental results at smaller angles will be discussed with special emphasis on the effects of charge cloud polarization.

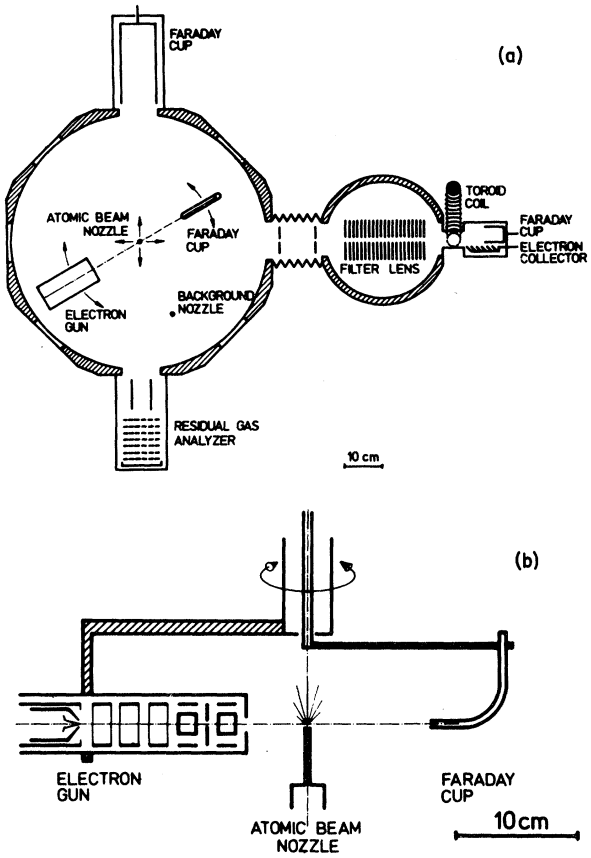

FIG. 1. (a) Horizontal cross section of the apparatus (schematic). (b) Vertical cross section of the scattering region of the apparatus (schematic).

Figures 1(a) and 1(b) show the arrangement of the subunits in the vacuum chamber. An electron gun and a Faraday cup are mounted on a rotating table. At the axis of the rotation, a capillary (1.8-mm i.d. and 50-mm length) produces the gas jet. This nozzle, as well as the Faraday cup, are adjustable in three dimensions. Scattered electrons enter an energy-filter lens that separates the inelastically and elastically scattered electrons. After leaving the filter lens, the elastically scattered electrons are deflected by the magnetic field of a solenoid. This prevents ions from reaching the detector, which is simply an electron collector attached to a vibrating reed electrometer.

The electron beam collides with the gas jet at the center of the scattering chamber, and the scattered electron intensity is recorded as a function of the scattering angle θ. A second set of scattering data is then collected using a second nozzle, equal to the first one except that its jet does not intersect the electron beam [see Fig. 1(a)]. This determines independently the contribution of the scattering from the background gas, which is subtracted from the first data set. The data were recorded on both sides of zero scattering angle to check for symmetry and to determine the zero scattering angle.

III. THE SCATTERING APPARATUS

A. The electron beam

Electrons are produced by a heated tungsten hairpin cathode and focused by a telefocus system. The telefocus system employs a relatively high anode voltage (2000–5000 eV) and a somewhat uncommon shape of the Wehnelt grid.[14] In common triode systems (an electron microscopy system, for example), a strong lens in front of the cathode produces a very small crossover of the electron beam, owing to the geometry of the Wehnelt grid. The disadvantage of the common arrangement is that the electrons interact strongly with each other in the crossover region. In unfavorable cases this may broaden the energy spread of the electron beam, formerly determined by the temperature of the filament, by about an order of magnitude (to approximately 2–5 V).[15] Furthermore, the major part of the emission current of the filament is blocked by the aperture system, so that only a small fraction of the emitted electrons form the final electron beam. With the Wehnelt grid geometry used in this experiment, the focusing lens in front of the cathode is weakened considerably and the crossover is moved into the Faraday cup 30

cm away from the filament. Thus the abnormal energy spread produced by the high charge density in the crossover of triode guns is avoided, and the ratio of emission current to beam current can be increased to near unity, depending on the aperture sizes. The shape and intensity of the electron beam are controlled by the distance from the Wehnelt cone to the rim of the Wehnelt cylinder, by the Wehnelt voltage, and by the anode voltage.

The electrons are decelerated to the final beam energy by an immersion system consisting of two cylinders and an aperture [see Fig. 1(b)]. It was found that these lenses must be aligned on the same cylindrical axis to better than 0.1 mm, since small deflections of the electron beam at the anode are magnified by the lenses which follow, producing an electron beam off the optical axis of the electron gun. Small misalignments can be corrected by means of deflector plates just in front of the gun. With the electron gun operating in a vacuum of about 1×10^{-5} Torr, an additional electron-beam focusing effect was observed, caused by the ions produced in the background gas at beam currents greater than 20 μA. Unfortunately, some ions were also produced in the deceleration stages, producing a very weak ionic beam which had to be removed in the detection system. The primary electron beam was trapped 12 cm behind the scattering volume by a Faraday cup. The Faraday cup was made from a bent tube (Wood Horn) so that electrons impinge on the inside wall at small incidence angles. The vast majority of the electrons are further deflected into the tube, and only a very small fraction of the electron beam is reflected backward into the scattering chamber. These Faraday cups are used in our laboratory at the University of Texas with great success in high-energy electron scattering (40 keV) and were found to be very efficient at low energies as well. The Faraday tube is 6 mm in diameter and has 0.1-mm-thick walls. All measurements presented here were made with at least 99% of the primary beam trapped in the Faraday cage and at most 1% remaining untrapped due to reflection, beam spread, etc. The electron-beam intensities were varied from 1 μA (for small angles and low energies) to 200 μA (for very large scattering angles and high energies).

B. The gas jet

A capillary of 1.8-mm I.D. and 50-mm length was used to produce a gas jet. Since the pressure in the gas reservoir behind this capillary was about 1–2 Torr (adjusted by a needle valve), the nozzle was not in the molecular (Knudsen) range. However, the electron beam was so well collimated that it was possible to make the electron beam and gas jet intersect 1 mm beyond the end of the capillary without appreciable nozzle scattering. Close to the end of the capillary, the gas density is much higher than the background gas density, and this provides a suitable scattering target. Figure 2 shows an atomic beam profile measured as the capillary was moved perpendicular to the detector (located for this measurement at 90° scattering angle). If the electron beam crossed the gas jet about 2 mm above the nozzle, the recorded full width at half maximum (FWHM) was 4.5 mm (convolution of the electron and the gas beams). Away from the center of rotation [see Fig. 1(a)], a second nozzle equal to the center one was mounted, to reproduce the background gas pressure in the chamber (which was around 10^{-5} Torr with the center nozzle running) for the background correction measurement. This procedure has two major advantages: first, the gas pressure in the scattering chamber, the electron beam, and its surrounding focusing ions remained constant. Second, if there is even a minute fraction of scattering from the center nozzle itself, both data sets will contain this contribution, which will be canceled in the evaluation of the data.

C. The filter lens and the detector

The purpose of this unit was to measure elastically scattered electrons only, so a filter lens was required to separate the electrons elastically and inelastically scattered within its acceptance, which had to be wide enough to be assured inclusion of the entire scattering volume in its acceptance cone. The selected design belongs to the group of *gegenfeld,* or retarding-field lenses. It had a parabolic electric field along its axis and was discussed in detail in Ref. 16. Its front aperture was 3 mm in

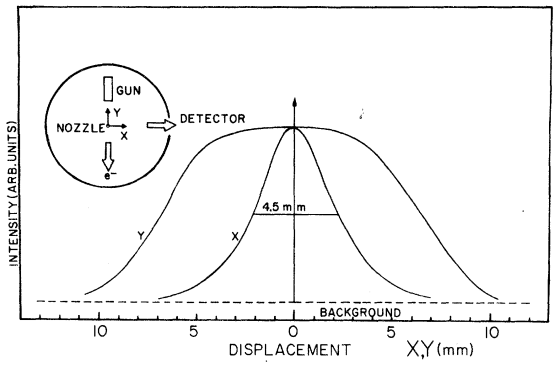

FIG. 2. Gas beam profile (X) and acceptance (Y) of the detection system. The insert shows the principle of the measurement (cf. text). The upper rim of the nozzle was 2 mm below the center of the electron beam.

diameter, followed by 21 plates with 10-mm holes. Its acceptance cone was measured. The results of these measurements are shown in Fig. 2. The acceptance cone profile (curve labeled Y) shows that the atomic beam (profile curve labeled X) is within the acceptance cone of the filter lens, so that no significant corrections have to be applied to the recorded data. Figure 3 shows an integral spectrum recorded with Xe as a scattering target. All of the data reported here were recorded with the retarding voltage set at the position indicated by the arrow in Fig. 3.

Although the filter lens very efficiently separates electrons scattered elastically from those scattered inelastically, it fails completely to eliminate positive ions. This could have easily falsified the $\sigma(\theta)$ curves, especially at very small scattering angles. To eliminate this problem, a toroidal coil was mounted just past the filter lens [as shown in Fig. 1(a)]. The magnetic field in the gap of the toroid deflected ions to the left and electrons to the right. An off-axis collector, constructed in venetian-blind configuration, was covered with graphite to ensure maximum efficiency in trapping the electrons. The ions were trapped in separate cages. The stray field of the toroid was not large enough to affect the efficiency of the filter lens. The final intensity of electrons in the Faraday cage was recorded by means of a vibrating reed electrometer.

IV. CALIBRATION OF THE APPARATUS

When all disturbing fields (electric and/or magnetic) had been either eliminated or compensated, a series of calibration measurements had to be made to ensure that the data would not be influenced by multiple scattering, focusing ions, angular resolution, scattering from the background gas, or faulty centering. The two (atomic and electronic) beams had to be adjusted simultaneously so that they crossed each other and that the crossing point was in the axis of rotation of the electron gun. The alignment procedure was performed as follows: the gun was rotated into position at 90° with respect to the detector, and the capillary (in a raised position) was moved horizontally perpendicular to the beam path until the electron beam was blocked from the Faraday cup by the capillary. The detector was turned to −90°, and the capillary was again moved horizontally to block the beam; the measured movement of the nozzle is twice the distance by which the electron beam missed the rotation center. The electron beam was redirected with a set of deflector plates to reduce this distance, and the whole procedure was repeated at these and other angular positions until the electron beam hit the nozzle at all angles. The nozzle was then lowered from the beam, and the axis of the filter lens was adjusted in order to center the scattering volume in the acceptance cone of the filter. Measurements similar to those shown in Fig. 2 were used to check the apparatus before taking data. To ensure that the scattered electrons entered the filter lens symmetrically, cutoff curves (shown in Fig. 3) were recorded. It was found that if the axis of the filter lens was at an angle to the path of the incoming electrons, the plateau in the cutoff curve disappeared.

After the alignment procedure had been performed, the nozzle was lowered until, with the background nozzle admitting gas, no scattering signal could be found originating from the main capillary. The final check was made by moving the main capillary horizontally (perpendicular to the electron beam). This yields a very sensitive test of any unwanted scattering from the upper rim of the nozzle. With the nozzle set in its centered position, the ratio of the scattered intensities, employing the two nozzles alternatively, was about 10 at midrange angles, decreasing to about 2 for the smallest angles; this is due to the angular dependence of the background scattering volume ("sine correction"). The smallest angle scattering of Ar with electron-beam intensities of 248, 28, 15, and 3.4 μA at 200-eV energy was recorded, and within the 3% experimental uncertainty, no difference in the cross sections could be observed, i.e., the effect of the electron-beam focusing by ions was imperceptible. Since the ion formation in hydrogen is weaker than in argon, ionic deflection of the electrons scattered at small angles was negligible.

Multiple scattering was investigated in the following way: the elastic scattering cross sections for Ar are much larger than those for H_2, so multiple-scattering effects were investigated for 600-eV

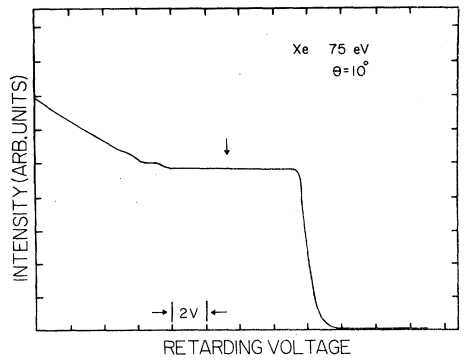

FIG. 3. Integral spectrum 75-eV electrons scattered from xenon, demonstrating the performance of the energy-filter lens. The arrow indicates the retarding voltage at which elastic cross sections have been measured.

TABLE I. Cross sections of electrons of H_2 in units of 10^{-19} cm^2 vs scattering angle in degrees.

θ (deg) \ E (eV)	100	200	400	600	1000
(0)	(8010)	(3375)	(1590)	(1180)	(1162)
3	5100	2100	1010	730	619
4	4400	1850	890	620	547
5	3780	1540	760	520	438
6	3280	1280	650	450	370
7	2850	1150	570	376	308
8	2450	960	500	320	252
9	2100	810	430	270	203
10	1820	720	380	231	171
12	1404	570	290	164	96
14	1170	440	220	119	60.8
16	950	350	160	79	37.0
18	790	275	116	53	25.0
20	652	221	85	37.6	17.5
24	440	143	47.7	20.6	11.7
28	320	91	28.5	12.6	6.5
32	230	60	18.2	8.5	4.4
36	161	41	12.7	6.1	3.0
40	117	26	9.5	4.7	1.9
45	78	19.5	7.1	3.2	1.15
50	56	14.1	5.1	2.3	0.76
55	41	10.7	3.8	1.53	0.54
60	30.8	8.4	2.8	1.12	0.395
65	24	6.8	2.1	0.82	0.31
70	18.8	5.85	1.57	0.62	0.25
80	13.2	4.07	0.99	0.42	0.16
90	10.2	2.93	0.68	0.30	0.104
100	8.5	2.11	0.50	0.212	0.079
110	7.0	1.61	0.39	0.176	0.063
120	6.1	1.30	0.32	0.141	0.049
130	5.4	1.07	0.27	0.117	0.0395

electrons scattered from argon, in order to magnify any effect. The scattered intensities at 10° and 25° were recorded for six different pressures. The ratios of the scattered intensities are shown in Fig. 4; the ratios should be constant as long as multiple scattering is negligible. Figure 4 shows that at pressures below 10^{-4} Torr, the scattering is free of multiple scattering within an error of ±3%. From the above it follows that the same is true for H_2.

From Fig. 2 it can be seen that the scattering volume had a diameter of about 4.5 mm or less, since our experiment measures a convolution of the electronic and atomic beams. Since the entrance slit of the filter lens (3 mm in diameter) was about 50 cm from the scattering volume, an upper limit of the acceptance angle was ±0.4°. This was the limiting factor in the angular resolution since the electron beam had a halfwidth of about 2 mm at the same distance. It was not necessary, however, to correct the data for angular resolution. A trivial calculation is sufficient to show that our exponential cross sections (the data show that this is a valid assumption) integrated over this angular uncertainty are approximately equal [within (2–3)%] to the corresponding integral, assuming a constant cross section, with the value of the exponential cross section at the center of that interval.

Our data contain a number of uncertainties. One set of experimental errors is independent of the shape of the $\sigma(\theta)$ curves, while another one depends strongly on the angular and energy dependence of the curves. Errors of the first kind are the fluctuations in intensity of the atomic and electronic beams (±3%) during a run of approximately two hours. A second source of uncertainty is the asymmetry between measurements on the right and left sides of the primary beam. In all data listed in Table I, measurements of the two sides agreed with each other to better than 3%, resulting in an estimated uncertainty for the averaged value of about ±2%. The strong angular dependence of the cross sections made switching of ranges inevitable in order to take measurements in the most sensitive range of the vibrating reed electrometer. In order to average the amplifier noise at the low intensities at large angles, the signals at each large angle was recorded for two minutes; the uncertainties introduced by switching the ranges and by the amplifier's noise are about ±2%. The angles were read off a large disk to $\frac{1}{5}$° precision, resulting in about ±1% error for the steep parts of the cross sections. The errors in the en-

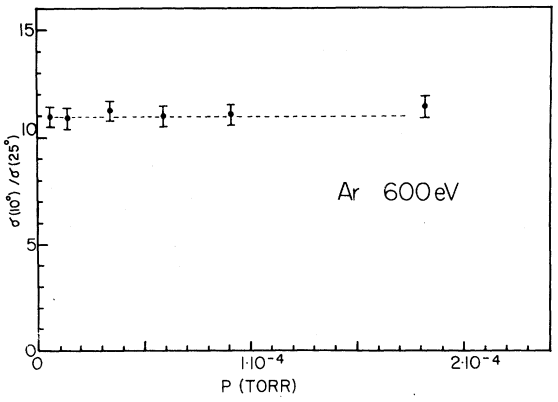

FIG. 4. Intensity ratios of scattered electrons taken at $\theta = 10°$ and 25° in argon at 600 eV vs pressure to check for multiple scattering. Although scattering from the atomic beam was employed, the pressure values given at the abscissa belong to the background pressure measured with an ionization gauge. The pressures within the atomic beam are much higher (cf. Fig. 2).

ergy determination (reading errors and contact potentials) will give rise to approximately ±3% error in shape. Since these are independent, they have to be added up quadratically, resulting in a total uncertainty of about ±5%.

There are, of course, some systematic error sources (especially at small angles). These are the finite angular resolution and the "wings" of the atomic beam, which are not contained in the acceptance angle of the detector system. Concerning the wings of the atomic beam and finite angular resolution, both will introduce an error of about 3% each at the smallest angles, with the tendency of the measured data to be too large there.

From the above discussion it follows that our estimated overall error in shape is ±5% and additionally 6% at small angles.[17] The absolute values given in Table I depend furthermore on the reliability of the theoretical values for $d\sigma/d\Omega$ at large angles which were used for the matching procedure. However, we are confident that this procedure is reasonable, because experiments agree very well in shape with the theoretical values.[18] If the theoretical large-angle values should be proven wrong, our data has to be rematched.

V. PRESENT DATA AND COMPARISON WITH PREVIOUS MEASUREMENTS

In 1970, Truhlar *et al.*[19] published a trilogy of papers giving a very detailed discussion of the H_2-e^- scattering process in the intermediate energy range (5–100 eV). Comparison of all current theories and experiments led them to conclude that the elastic DCS and the total elastic cross section σ_{tot} can be adequately described by first-order calculations, providing a polarization potential and exchange are included in the evaluation. A word of caution was added that there were indications that the adiabatic approach might break down at energies above 100 eV. This idea was reemphasized by the comparison of calculations by Ford and Browne[20] (which neglected polarization altogether) and Liu and Smith[21] with the measurements of Ulsh *et al.*[22] taken at 25 keV. This comparison shows that at this high energy the influence of charge cloud polarization had disappeared completely, and excellent agreement was reported after binding contributions had been taken into account.

Figure 5 shows our matched data as a function of the momentum transfer $s\,[=(4\pi/\lambda)\sin(\theta/2)]$. The independence of the cross section $\sigma(s)$ from the incident energy demonstrates the validity of the first Born approximation to very low energies, provided the scattering potential is sufficiently weak.

It should be noted once more that these data are superior to all previously reported data in at least two respects. First, the beam-beam geometry avoids any lengthy and uncertain "sine correction" for a variable scattering volume. Second, the angular range has been extended so that matching and interpretation becomes more reliable and the effect of the charge cloud polarization becomes more visible. Figure 6 shows our data in the small-angle range. We find an exponential slope in the DCS at small angles.

Finally, the differential cross sections were integrated over all angles and total cross sections were obtained. Figure 7 shows the total cross section as a function of energy, along with the values given by Truhlar *et al.*[19] The continuity between data sets is another indication of the validity of the matching procedure we have chosen for our data. Since the charge cloud polarization is predominantly a small-angle phenomenon, σ_{tot} will be less sensitive to polarization because small-angle contributions are weighted by the factor of $\sin\theta$.

VI. COMPARISON WITH THEORY AND CONCLUSIONS

In general, experimental cross sections of molecules are compared with calculations based on the independent-atom model.[23] In this approximation, the molecular scattering intensities are constructed by the coherent superposition of the constituent atomic intensities in the molecular configuration. This model disregards the rearrangement of the electron cloud during the formation of bonds. It was found that this approximation fails to predict small-angle cross sections by a significant amount, and the binding effects have to be properly taken into account in this range.[24] Fortunately, there are several very good calculations for H_2 which utilize molecular configuration interaction (CI) wave functions. A comparison of those theoretical results with measurements is shown in Figs. 5 and 6. The results are given in units of the momentum transfer s (instead of the scattering angle θ), since in this presentation the $\sigma(s)$ curves become energy independent as long as the first Born approximation is valid. Figure 5 shows very convincingly that all the large-angle data lie on a common curve, and that this line coincides with the prediction of Ford and Browne.[20] However, at small angles strong deviations can be seen. These deviations are caused by two phenomena which were neglected in the theory: first, the distortion of the molecular electronic cloud by the Coulombic field of the incoming electrons; second, the exchange of the incoming electron with the molecular electrons. If the exchange-scattering contribution is determined by an approximation used by Khare

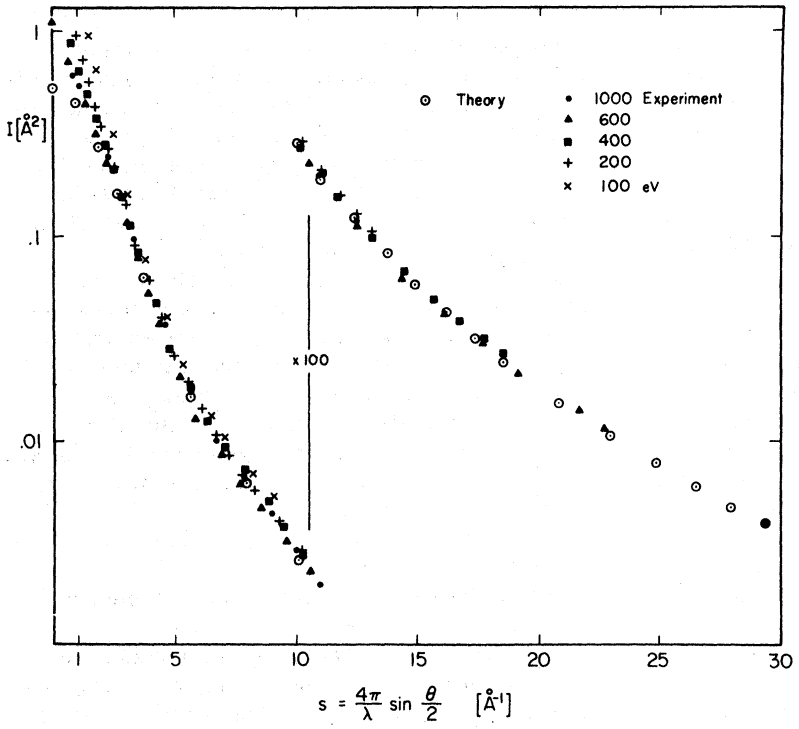

FIG. 5. Differential cross sections of electrons elastically scattered by H_2 vs momentum transfer $s = (4\pi/\lambda)\sin(\theta/2)$.

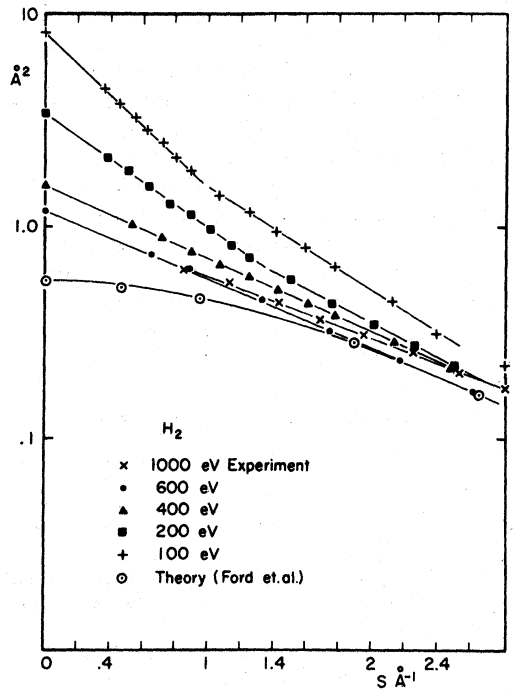

FIG. 6. Differential cross section of electrons elastically scattered by H_2 vs momentum transfer $s = (4\pi/\lambda)\sin(\theta/2)$.

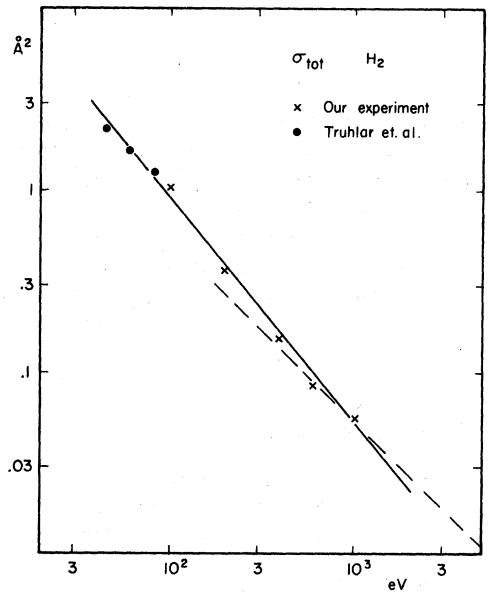

FIG. 7. Total elastic cross sections of electrons scattered by H_2 vs energy. The dotted line represents an application of a theory given by Inokuti *et al.* (Ref. 26) to H_2.

and Moiseiwitsch[25] and is added to the calculated values of Ford and Browne, a very large discrepancy still remains which must finally be attributed to the charge cloud polarization.

If the electronic charge cloud would be polarized adiabatically under the influence of the incoming electron, the static molecular potential V_{stat} has to be increased by an additional scattering potential V_{pol}. If the first Born approximation is valid (which is implied by the large-angle data given in Fig. 5), then the scattering amplitudes should still be energy independent when plotted as a function of the momentum transfer s. Such behavior was observed, for instance, by Truhlar *et al.* in their H_2 results for energies below 81.6 eV. At the energies we have investigated, such behavior could not be found for H_2. The $\sigma(s)$ at small angles changes drastically with energy, and this leads to the conclusion that in H_2 the adiabatic limit is reached below 100 eV. This limit of validity for adiabatic charge cloud polarization for H_2 was expected, since the static polarizability α is very large for H_2.

The present total cross sections are consistent with the "quasi" absolute measurements of Ulsh *et al.*,[22] when the results are compared to the theory by Inokuti and McDowell.[26] According to this theory, the total cross section is given by

$$\sigma_{tot} = \pi Z^2 k^{-2}(A + Bk^{-2} + \cdots),$$

$$A = 8\int_0^\infty |Z - F(s)|^2 s^3\, ds,$$

where $Z = 1$, F is the x-ray form factor, and k is the wave vector of the incoming electron. Ulsh *et al.* determine σ_{tot} to be 0.00197 Å^2 for H_2. Under the assumption that $B = \cdots = 0$, A is determined to be 4.2. When σ_{tot} is evaluated at the low energies at which the present data are determined, then very nice agreement is found for the three highest energies. However, at 100 eV, the experimental value exceeds the theoretical one by several standard deviations. This can be explained as a failure of the first Born approximation and is probably caused by the influence of the charge cloud polarization σ_{tot}. The dotted line in Fig. 7 shows the results of Inokuti's theory matched to Ulsh *et al.* and extrapolated to low energies.

It should be noted that all of the above conclusions, which were drawn from the comparison of experiment and theory, involve theories which disregard the influence of vibrational excitations. The neglect of these excitations is based on the theoretical results of Truhlar *et al.* and Ford and Browne, who found that the combined effects of all vibrational excitations contribute less than 1% to the total cross section at energies above 81.6 eV, and that this contribution comes mainly from large-angle scattering.

Note added in manuscript. After completion of this manuscript we learned of similar work by C. R. Lloyd *et al.*[27] Their measurements agree very well with ours for the overlapping energies and angles as well in shape and in absolute values.

ACKNOWLEDGMENTS

One of us (M. F.) is indebted to Professor J. Kessler and his co-workers of the Lehrstuhl für Experimentelle Atomphysik for their warm hospitality at the Westfälische Wilhelms Universität at Münster (Germany) while the experimental portion of the work was carried out. We would like to thank especially Dr. C. B. Lucas for making a substantial part of the equipment available to us. We are also grateful to the machinists of the machine shop for their reliable work. Finally, we want to acknowledge the support of the Deutsche Forschungsgemeinschaft.

---

†This work was supported in part by the Robert A. Welch foundation.

[1]L. J. Kieffer, At. Data 2, 293 (1971).
[2]J. Kessler, Rev. Mod. Phys. 41, 3 (1969).
[3]F. J. Mehr and M. Wilmers, Uni. Nat. de Colombia, Bogota, Colombia (private communication).
[4]H. F. Wellenstein, R. A. Bonham, and R. C. Ulsh, Phys. Rev. A 8, 304 (1973).
[5]D. Golden and H. Bandel, Phys. Rev. 149, 58 (1966).
[6]L. J. Joachain and C. Quigg, Rev. Mod. Phys. 46, 279 (1974).
[7]S. Westin, K. Nor. Vidensk. Selsk. Skr. 2, 1 (1946).
[8]G. E. Chamberlain, S. R. Mielczarek, and C. E. Kuyatt, Phys. Rev. A 2, 1905 (1970).
[9]J. P. Bromberg, J. Chem. Phys. 50, 3906 (1969); J. Chem. Phys. 61, 963 (1974).
[10]L. Vriens, C. E. Kuyatt, and S. R. Mielczarek, Phys. Rev. 170, 163 (1968).
[11]E. A. Silverstein, Nucl. Instrum. Methods 4, 53 (1959).
[12]T. W. Shyn, R. S. Stolarski, and G. R. Carignan, Phys. Rev. A 6, 1002 (1972).
[13]M. Fink and A. C. Yates, At. Data 1, 385 (1970).
[14]K. H. Steigerwald, Optik (Stuttg.) 5, 469 (1949).
[15]D. Hartwig and K. Ulmer, Z. Phys. 173, 294 (1963).
[16]H. D. Zeman, K. Jost and S. Gilad, Rev. Sci. Instrum. 42, 485 (1971).
[17]In principle, our results could be corrected for the small-angle effects. This is not done, however, in Table I. Without correction, the total uncertainty will be ±8%.

[18]P. Moore and M. Fink, Phys. Rev. A 5, 1747 (1972).
[19]D. G. Truhlar and J. K. Rice, J. Chem. Phys. 52, 4480 (1970); S. Trajmar, D. G. Truhlar, and J. K. Rice, J. Chem. Phys. 52, 4502 (1970); S. Trajmar, D. G. Truhlar, J. K. Rice, and A. Kupperman, J. Chem. Phys. 52, 4516 (1970).
[20]A. L. Ford and J. C. Browne, Chem. Phys. Lett. 20, 284 (1973).
[21]J. W. Liu and V. H. Smith, Jr., J. Phys. B 6, L275 (1973).
[22]R. C. Ulsh, H. R. Wellenstein, and R. A. Bonham, J. Chem. Phys. 60, 103 (1974).
[23]H. Kambara and K. Kuchitsu, Jpn. J. Appl. Phys. 11, 609 (1972).
[24]M. Fink, R. A. Bonham, and D. A. Kohl, J. Chem. Phys. 52, 5487 (1972).
[25]S. P. Khare and B. L. Moiseiwitsch, Proc. Phys. Soc. Lond. 85, 821 (1965).
[26]M. Inokuti and M. R. C. McDowell, J. Phys. B 7, 2382 (1974).
[27]C. R. Lloyd, P. J. O. Teubner, E. Weigold, and B. R. Lewis, Phys. Rev. A 10, 175 (1974).